SYNTHESIS AND PHYSICOCHEMICAL STUDY OF GUM ARABIC SULFATES

ALEKSANDR S. KAZACHENKO,[*,**], FERIDE AKMAN,[***] UTKIRJON HOLIKULOV,[****] YAROSLAVA BEREZHNAYA,[**] NOUREDDINE ISSAOUI,[§] ANNA S. KAZACHENKO,[*] OMAR M. AL-DOSSARY,[§] OLGA FETISOVA,[**] SVETLANA NOVIKOVA[**] and TIMUR IVANENKO[**]

[*]*Siberian Federal University, pr. Svobodny 79, Krasnoyarsk 660041, Russia*
[**]*Institute of Chemistry and Chemical Technology, Krasnoyarsk Science Center, Siberian Branch, Russian Academy of Sciences, Akademgorodok 50/24, Krasnoyarsk 660036, Russia*
[***]*Vocational School of Food, Agriculture and Livestock, University of Bingöl, Bingöl 12000, Turkey*
[****]*Department of Optics and Spectroscopy, Samarkand State University, 15 University Blvd., Samarkand 140104, Uzbekistan*
[§]*Laboratory of Quantum and Statistical Physics, Faculty of Sciences, University Monastir, 5079, Tunisia*
[§]*Department of Physics and Astronomy, College of Science, King Saud University, PO Box 2455, Riyadh, 11451 Saudi Arabia*
✉ *Corresponding author: A. S. Kazachenko, leo_lion_leo@mail.ru*

Received May 19, 2024

Polysaccharide sulfates have many valuable types of biological activity, such as anticoagulant, hypolipidemic, antithrombotic, *etc*. The biological activity of sulfated polysaccharides depends on various physicochemical characteristics. In this work, the synthesis and physicochemical characteristics of gum arabic sulfates were studied. Sulfation of gum arabic was carried out with sulfamic acid in the presence of urea with varying ratios of the sulfating complex. The influence of process duration and temperature on the sulfur content in gum arabic sulfates was assessed. The original and sulfated gum arabic was studied using a complex of physicochemical methods: FTIR, XRD, thermal and elemental analysis and DFT. The introduction of a sulfate group into the gum arabic macromolecule was proven by FTIR spectroscopy by the appearance of corresponding absorption bands. According to thermal analysis, during the sulfation process, the thermal stability of gum arabic decreases due to the formation of low-stable sulfuric acid ester groups.

Keywords: gum arabic, sulfamic acid, physicochemical characteristics, DFT

INTRODUCTION

Gum arabic (GA) is a dried exudate obtained from the stems and branches of the acacia tree (Acacia Senegal or Acacia Seyal). It is a mixture of galactose, arabinose, rhamnose, glucuronic acid, their salts and glycoproteins, and has a highly branched structure. Chemically, GA is a complex mixture of macromolecules of different sizes and compositions, which includes morphological structures in the form of compact arabinogalactan protein and disc arabinogalactan.[1] Some authors believe that natural gum arabic has the shape of a flower, where petals formed by polysaccharide macrocycles are strung on a polypeptide chain.[2]

The polysaccharide backbone consists of 1,3-linked galactopyranosyl residues substituted at the O-2, O-6 or O-4 positions. The side chains consist of two to five 1,3-linked β-D-galactopyranosyl units connected to the main chain by 1,6-linkages. Both the main and side chains contain α-L-arabinofuranosyl, α-L-rhamnopyranosyl, β-D-glucopyranosyl and 4-O-methyl-β-D-glucopyranosyl units, the latter two most often being the terminal units.[3] The chemical composition of GA varies depending on origin, climate, harvest season, tree age and processing conditions.[4] GA is used industrially due to its

exceptional properties, such as antioxidant properties and antimicrobial activity.

Physicochemical modifications of gum arabic have been little studied. Basically, it is subjected to thermal and mechanical treatment to increase its emulsifying ability. Chemical modifications of gum arabic include: removal of metal ions and production of arabic acid,[5,6] interfacial polycondensation with terephthalic acid dichloride, interaction with epichlorohydrin, epoxy resins, butyric and glutaraldehydes.[7-10]

For most polysaccharides, other modifications are also known, in particular sulfation. In addition to functional properties, sulfated polysaccharides demonstrate antiviral, antiparasitic, antiatherosclerotic, anticoagulant and antithrombotic and other activities.[11] That is why, the development and production of new sulfated products from food polysaccharides is a promising area of chemistry.

Sulfation is the nucleophilic substitution of hydroxyl groups of polysaccharides and the production of their esters. Many methods have been developed for the synthesis of polysaccharide sulfates. However, most of them involve the use of toxic and dangerous reagents, which leads to complications in the technological process, premature corrosion of equipment and severe destruction of the original polymer. The efficiency of sulfation is influenced by the nature of the polysaccharide, the composition of its monomers and the configuration of glycosidic bonds, molecular weight and other structural factors. Even for the same polysaccharide, the reaction results depend on the sulfating agent, the ratio of components, the medium, the time and temperature of the reaction.[12]

In the studies of Torlopov,[13,14] the sulfation of polysaccharides with chlorosulfonic acid ($ClSO_3H$) in pyridine was carried out. In the study of Wang,[15] the synthesis methods, structure, and anticoagulant activity of the MCC sodium salt were discussed. The MCC sulfation carried out with the $ClSO_3H$–dimethylformamide complex under different conditions yielded products with different DS values. Other studies[16,17] were devoted to the use of ionic liquids, including 1-butyl-3-methylimidazolium chloride, 1-allyl-3-methylimidazolium chloride, and 1-ethyl-3-methylimidazolium acetate, as reaction media for homogeneous sulfation and as solvents for cellulose. Sulfation was performed with $ClSO_3H$ or the complexes of SO_3 with dimethylformamid (DMF) or pyridine in the ionic solution at 25 °C. In the solution of 1-ethyl-3-methylimidazolium acetate, acetylation occurred instead of the expected SC formation due to the participation of acetate ions in side reactions.

The H_2SO_4, SO_3, and $ClSO_3H$ compounds widely used in the sulfation reactions are highly aggressive reagents, which require special equipment and thereby complicate the process. In contrast to the above-listed reagents, sulfamic acid (NH_2SO_3H) is a stable nonhygroscopic crystalline substance. Its strength as an acid is comparable with that of H_2SO_4. Sulfamic acid is commercially manufactured by reacting urea with oleum.

Currently, the process of searching for less toxic reagents for sulfation is underway in order to reduce the danger of production, reduce costs and reduce the number of stages of purification of the original product. Such a promising reagent is sulfamic acid, which is used in our work. The purpose of this work was to synthesize gum arabic sulfates using a new method and to study the physicochemical characteristics of the resulting products.

EXPERIMENTAL

Sulfation of gum arabic

Pure gum arabic produced by Sigma-Aldrich was used as the starting raw material.

Sulfation of gum arabic was carried out with sulfamic acid in 1,4-dioxane in the presence of urea. To do this, 50 mL of dioxane, 4.9-12.1 g (50-125 mmol) of sulfamic acid and 3.1-7.8 g (50-125 mmol) were placed in a three-neck flask equipped with a thermometer, a mechanical stirrer and a water bath. Urea, the resulting mixture, was heated with vigorous stirring to 50 °C and 5 g of air-dried gum arabic was added to it. Then, the temperature of the reaction mixture was raised to a fixed value (in accordance with the sulfation conditions given in Table 1) and stirred at this temperature for 1-4 hours. At the end of sulfation, the solvent was decanted, and the resulting viscous residue was dissolved in 25 mL of water, the excess sulfamic acid was neutralized with a 25% aqueous solution of ammonia until neutral.

The ammonium salt of sulfated gum arabic was purified by dialysis on cellophane against distilled water. The product was dialyzed for 10 hours, changing the water at intervals of 1-2 hours.

Physico-chemical analysis of samples

The content of sulfur in the resulting GA sulfate ammonium salts was found using a Flash EATM-112 elemental analyzer (ThermoQuest, Italy).

FTIR spectra of initial and sulfated GA were obtained on a Shimadzu IRTracer-100 FTIR spectrometer (Japan) at wavelengths within 400–4000 cm^{-1}. The spectra were then identified in the OPUS

software, version 5.0. Tablet-shaped solid specimens for the FTIR study contained 2 mg of a substance per 1000 mg of KBr.

The X-ray diffraction study was carried out on a DRON-3 X-ray diffractometer (monochromatic CuK_α radiation, λ = 0.154 nm) at a voltage of 30 kV and a current of 25 mA. The scanning step was 0.02 deg and the intervals were 1 s per data point. The measurements were performed in the range of the Bragg angles 2Θ from 5.00 to 70.00˚.

Thermal analysis was carried in a corundum crucible using an STA 449 F1 Jupiter instrument (Netzsch) in the temperature range from 30 to 900 °C (the heating rate was 10 °C/min) in an argon flow (the shielding and purge gas flow rates were 20 and 50 mL/min, respectively). The measurement data were processed using the Netzsch Proteus Thermal Analysis 5.1.0 software package supplied with the instrument.

NMR spectra were recorded on a Bruker Avance 600 instrument (Bruker, Germany) in standard 5 mm NMR ampoules. To stabilize the signal, 15 μL of D_2O were added to the studied solutions. 1H spectra were recorded using a single pulse at an operating frequency of 600 MHz with a relaxation delay of 5 μs. The standard zgpr pulse sequence from the Bruker library was used to suppress the water signal. 13C{1H} spectra with proton decoupling were recorded at an operating frequency of 150 MHz with a relaxation delay of 6.5 μs, with the accumulation of 512 scans for 19 h. Chemical shifts are presented relative to the signal of the deuterium solvent (D_2O). All spectra were processed using the Topspin 3.2 software package.

Quantum chemical calculation

The optimization and quantum chemical calculations of GA and GA sulfate molecules were performed using the B3LYP/6–31G(d, p) DFT technique in the Gaussian 09 and GausView 5.0 software program.[23,24] Fukui functions ($f^+(r)$, $f^-(r)$, $f^0(r)$, and $\Delta f(r)$) were determined using the Multiwfn multifunctional program.[25]

RESULTS AND DISCUSSION

Synthesis of gum arabic sulfates (GA-S)

Chemically, gum arabic is a high molecular weight polysaccharide arabinogalactan.[26] Due to the similarity of chemical composition and differences in molecular weight, the process of sulfation of gum arabic can be compared with the process of sulfation of arabinogalactan from larch wood.[27] Despite the fact that currently the processes of sulfation with sulfamic acid are actively developed and modified,[28,29] the process of sulfation of polymers with sulfamic acid in 1,4-dioxane in the presence of urea can be considered quite popular.[30-32]

A promising sulfating agent, closely related to complexes of SO_3 with bases (which are traditionally used for the synthesis of polymer sulfates), is sulfamic acid, which can be considered as a $SO_3{\cdot}NH_3$ complex.[12,33-35] As a rule, sulfamic acid, when heated with alcohols, forms sulfates in the form of the corresponding ammonium salts, according to the reaction:

$$ROH + NH_2SO_3H \longrightarrow ROSO_3NH_4 \quad (1)$$

In terms of properties in sulfation and sulfonation reactions, sulfamic acid is close to SO_3-tertiary amine complexes. In industry, the interaction of sulfamic acid with alcohols in the presence of catalysts, such as organic bases, is used to reduce the temperature of sulfation processes.[12,33-35] In this work, urea was used as the most effective activator of the process.[32] The results on the effect of sulfation process conditions on the sulfur content in gum arabic sulfates are given in Table 1.

According to the data presented in Table 1, the degree of GA sulfation increases both with an increase in the process temperature from 70 °C to 95 °C, and with an increase in its duration from 1 to 4 hours. It was found that reducing the ratio of GA: sulfating complex to 1:10 (g:mmol) leads to a sharp decrease in the sulfur content, even at high temperatures and duration of the process.

It has been shown that a high sulfur content of GA (above 12 wt%) is achieved when the sulfation process is carried out for 2.0-3.0 hours at a temperature of 85-95 °C with a reagent ratio (HA:SA) of no less than 1:14 (g:mmol). It should be noted that similar sulfation conditions when using arabinogalactan from larch wood as a feedstock led to the production of sulfated products with a lower sulfur content in the resulting product (up to 12 wt%).[27] This may be due both to the activity of polysaccharide hydroxyl groups in the sulfation reaction and to their accessibility to the sulfating agent.

FTIR analysis

The introduction of a sulfate group into the gum arabic macromolecule was confirmed by IR spectroscopy data (Fig. 1). The presence of absorption bands at 806 cm^{-1} and 860 cm^{-1}, which are absent in the IR spectrum of the original gum arabic, indicates the presence of primary and secondary sulfates of the ammonium salt of gum arabic. In the FTIR spectra of sulfated samples, there is a decrease in the intensity of the absorption band of stretching vibrations of hydrogen-bonded

OH groups in the region of 3600-3000 cm^{-1} and the absorption band of planar deformation vibrations of OH groups at 1327 cm^{-1}, which indicates a decrease in the number of OH groups in the sulfated product, due to their partial replacement with SO_3 groups. The IR spectrum of sulfated gum arabic also contains a wide high-intensity band at 1249 cm^{-1}, corresponding to vibrations of the sulfate group. It should be noted that gum arabic consists of the monosaccharides arabinose and galactose, which makes it structurally similar to arabinogalactan; one of the differences is the length of the macromolecular chain and, accordingly, the molecular weight. When comparing the FTIR spectra of gum arabic sulfate with arabinogalactan sulfates obtained by various methods,[27,29,36-38] patterns similar to those described above are observed.

Table 1
Sulfur content in the products of sulfation of gum arabic with sulfamic acid in 1,4-dioxane environment

№	Temperature, °C	Time, h	GA/SC Ratio, g:mmol	Sulfur content, wt%
1	70	2.5	1:30	2.7
2	80	1	1:14	1.8
3	80	2	1:14	6.9
4	80	3	1:14	7.5
5	80	3	1:30	8.8
6	80	4	1:30	10.1
7	85	2	1:14	9.7
8	85	2.5	1:14	11.1
9	85	3	1:14	11.5
10	85	3	1:20	12.8
11	90	2	1:20	12.9
12	90	2.5	1:20	14.8
13	90	3	1:20	15.3
14	95	2.5	1:10	5.3
15	95	2.5	1:14	12.4

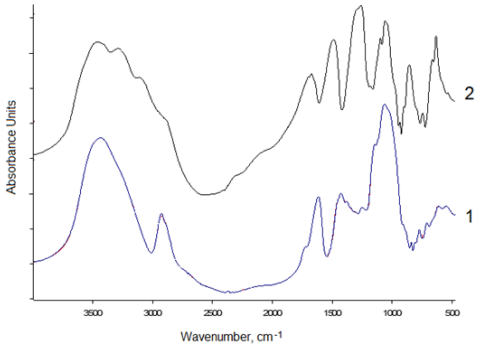

Figure 1: Experimental FTIR spectra: 1 – gum arabic, 2 – gum arabic sulfate

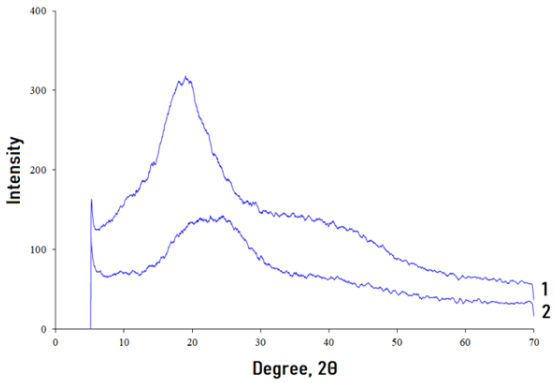

Figure 2: X-ray diffraction patterns: 1 – gum arabic, 2 – gum arabic sulfate

XRD

Natural polysaccharides have different crystallinity and can be divided into crystalline and X-ray amorphous. Crystalline include cellulose[39] and xylan,[40] and X-ray amorphous include guar gum,[41,42] xanthan,[30] arabinogalactan,[36] galactoglucomann,[31] agarose[43] and some others.[44,45] Gum arabic can be classified as an X-ray amorphous polysaccharide.[46,47] During the sulfation of gum arabic, its X-ray amorphisation increases, as indicated by a decrease in the halo in the region from 10 to 30˚ 2Θ (Fig. 2). The results obtained are consistent with data on the sulfation of other polysaccharides.[48,49]

NMR

Arabic gum

The signals at 1.17, a doublet at 1.24 (J=6.24 Hz), and a doublet of doublets at 1.36 (J=7.18, 3.25 Hz) are attributed to methyl groups attached to

sugars, such as in rhamnose or other deoxy sugars.[50] The doublet and doublet of doublets suggest that these protons are bound to adjacent methylene groups, consistent with methyl protons on sugar units (Fig. 3). The slightly broadened singlets at 2.03 ppm and 2.12 ppm indicate that these protons are attached to adjacent methylene groups, consistent with methyl protons on sugar units. Protons are possibly from amino acid residues in the protein component of gum arabic or attached to sugar residues, such as uronic acids (*e.g.*, glucuronic acid).[51] Alternatively, the broadening of the signals may be due to signal overlap due to the polymeric nature of the substance. The group of signals in the 3.0-4.5 ppm region corresponds to protons attached to C2-C5 in sugar rings, typical of carbohydrate structures. The overlap suggests a mixture of different sugar residues, including arabinose, galactose, rhamnose, and glucuronic acid, which are known components of gum Arabic.[52] The signals in the 4.9-5.5 ppm region indicate anomeric protons (attached to C1 in sugar units). Multiple closely spaced peaks suggest the presence of several types of glycosidic bonds, both α- and β-anomers.[53]

The ^{13}C NMR spectrum shows a characteristic signal of the methyl group of rhamnose (20.14 ppm). The signals around 48 ppm are due to the methylene groups in the sugar rings (48.03, 48.17, 48.30). The signals in the 60-76 ppm region correspond to carbons C2-C5 and are typical of polysaccharides. The large number of peaks reflects the heterogeneity of sugar residues present in gum arabic. The signals 79.0-82.5 probably correspond to carbons C3 and C4 of uronic acids or oxygenated carbons in sugar units that are more heavily substituted or involved in glycosidic bonds. This region is also characteristic of branched sugars. The group of signals 97.5-104.5 ppm corresponds to anomeric carbons (C1), the multiplicity of signals reflects different types of glycosidic bonds (both α- and β-anomers) in the polysaccharide. The signals at 175-177 ppm correspond to carbonyl carbons, probably from carboxyl groups in uronic acids or esterified groups in the structure of gum arabic.[54]

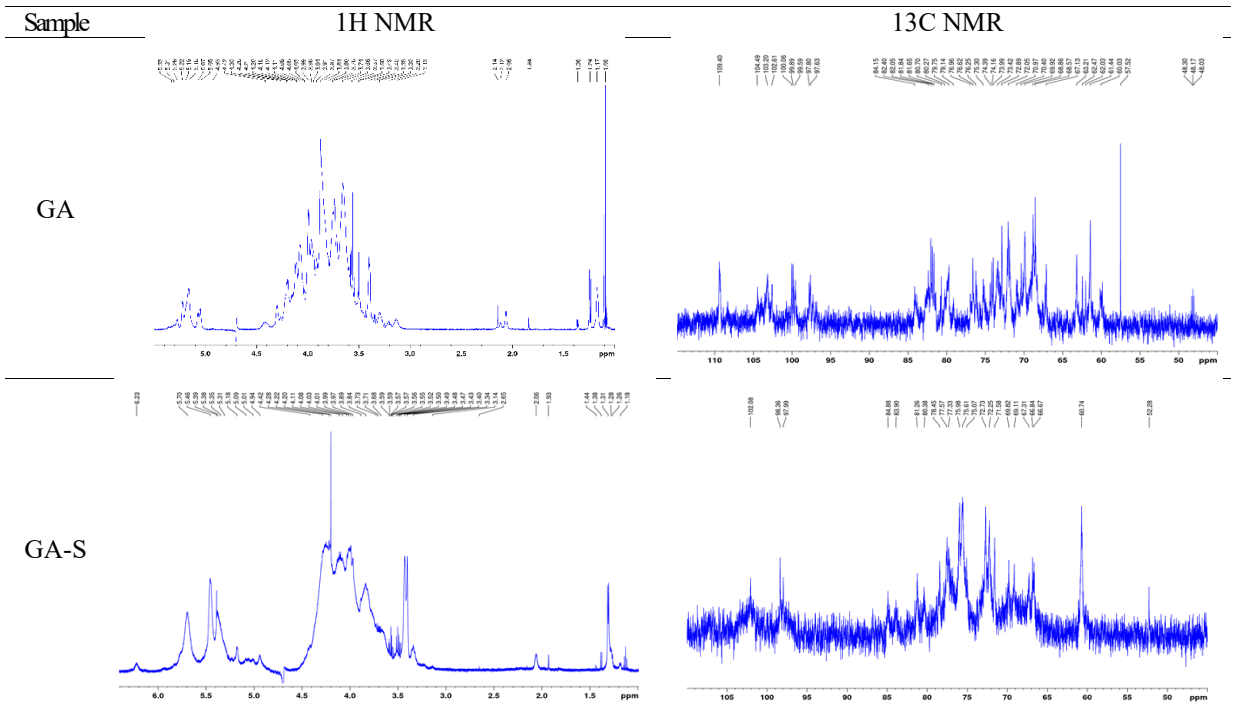

Figure 3: NMR spectra of arabic gum (GA) and arabic gum sulfate (GA-S)

Sulfated arabic gum

A slight shift of the signals of methyl groups is observed in the 1H spectrum of gum sulfate from 1.18 to 1.30 ppm, as well as a significant decrease in their intensity, which indicates a lower content of rhamnose or other methyl-containing sugars in the sulfate. The broadened signals of uronic acids at 1.93 and 2.06 ppm are preserved, although they are slightly shifted relative to the signals in the original gum. The signals of C2-C5 protons in the range of 3.0-4.5 ppm are preserved, but have undergone significant changes in intensity: a clear decrease in the intensity of the signals at 3.0-3.9 ppm and an increase in the intensity at 4.0-4.6 ppm

are observed. This indicates changes in the environment of the hydroxyl group and potential sulfation at positions C2, C3 or C4 of the sugar rings. The shift of the signals of anomeric protons in the range of 5.1-5.8 ppm is also associated with the redistribution of electron density during sulfation, and the change in signal intensities indicates possible sulfation of the C1 atoms.

The appearing broadened and low-intensity signals at 6.20 and 7.02 ppm probably correspond to sulfated sugar residues, possibly reflecting the C-O-S bond. In the 13C NMR spectrum, a new signal appears at 52.3 ppm, which may correspond to the C1 or C6 atoms of the sulfated gum. The signals in the range of 60.5-80.5 ppm are still present, but changes in their positions and intensities suggest changes in the sugar backbone due to sulfation. The new peak positions probably reflect sulfation at C2, C3 or C4 of the sugar units, in particular the galactose or glucuronic acid residues. The signals at 98.0-104.5 ppm still correspond to anomeric carbon atoms, although small shifts indicate that sulfation has also affected the anomeric centers. A new signal appears at 162.86 ppm, characteristic of carbon atoms linked to the sulfo group. The signals of the carboxyl carbon from the uronic acid residues (174-177 ppm) are preserved, indicating that sulfation did not have a significant effect on these groups.

TGA/DSC analysis

The results of thermal analysis, with the TG and DSC thermograms of the original and sulfated gum arabic, are shown in Figure 4. The characteristics of the thermal decomposition process of the studied compounds are presented in Table 2.

The analysis of the obtained TG curves shows that the weight loss during thermolysis of the original GA occurs in three stages. At the beginning of heating and up to 170 °C, moisture and low molecular weight substances are removed. The wide temperature range of this process can be explained by the difficulty of breaking hydrogen bonds between water molecules and polar functional groups of polysaccharides.[55,56] In this case, the sample loses 6.2% of the initial sample. On the DSC curve, this temperature range corresponds to the endo-effect, which corresponds to the removal of adsorption water.

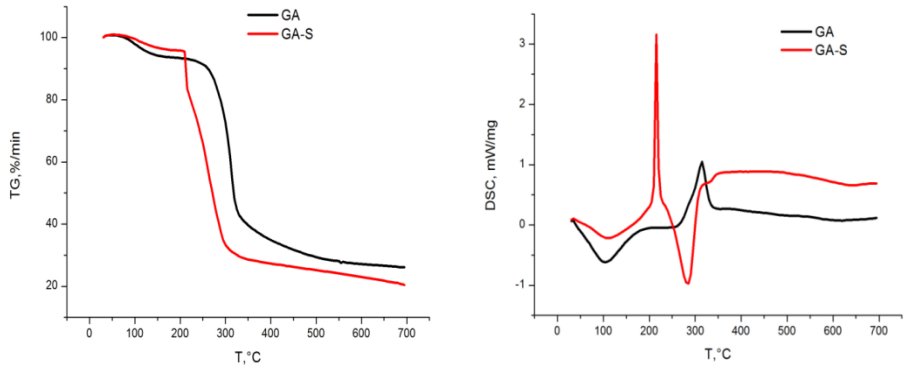

Figure 4: TG and DSC curves of original and sulfated gum arabic

Table 2
Characteristics of thermogravimetric analysis of original and sulfated gum arabic

Sample	Decomposition stage number	Temperature range, °C	Weight loss, %	Activation energy, kJ/mol	Remaining at 700 °C, %
GA	1	30-170	6.2	-	-
	2	250-330	48.5	86.5	-
	3	330-700	16.9	-	26.1
GA-S	1	30-170	3.8	-	-
	2	200-215	12.1	-	-
	3	215-300	50.5	49.5	-
	4	300-700	12.7	-	20.5

The loss of moisture for the sulfated sample GA-S occurs in the same temperature range (from 30 to 170 °C), while the weight loss is less (-3.8%) than that of the original sample. The thermal effect

that characterizes this stage of thermolysis also occurs in the endothermic region, but with less intensity. The main decomposition of the original GA begins after 250 °C and continues up to 330 °C, which is consistent with the thermal destruction of most biopolymers.[57] During this heating stage, the main weight loss of the sample occurs, up to 48.5%. The main decomposition of GA is accompanied by the release of heat, which is characterized by an exothermic effect on the DSC curve (Fig. 4). It is generally accepted that in this temperature range, competing reactions, such as dehydration, depolymerization and decomposition of organic matter, occur, leading to the formation of H_2O, CO and CH_4.[58,59] With further heating up to 700 °C, carbonisation of the structure occurs, with the formation of char (weight loss 16.9%).

The mechanism of the main stage of thermolysis of the sulfated sample, in contrast to the original GA, occurs in two stages. Initially, in the range of 200-215 °C, the TG curve tends almost vertically downward, with a weight loss of 12.1%. On the DSC curve, this interval corresponds to a sharp and rather intense exothermic peak, with a maximum at 215 °C. It is likely that at this stage of GA-S thermolysis, the formation of sulfuric acid molecules occurs as a result of the interaction of two closely located sulfate groups belonging to different macromolecules according to the reaction $ROSO_3H + HO_3SOR = RO_2SO_2R + H_2SO_4$.

With further heating up to 300 °C, intense loss of sample weight continues, up to 50.5% of the initial sample. The DSC curve of this interval passes into the endothermic region. A possible explanation for the endothermic nature of this stage is the thermal destruction of the structure of the substance. A similar two-stage decomposition of the main stage of thermolysis of sulfated cellulose was noted in works.[60,61] During the final stage of thermolysis (300-700 °C), the weight loss of the sulfated sample was less intense (12.7%).

It is generally accepted that the temperature at which the main decomposition of a substance begins characterizes its thermal stability.[58,59] Based on thermogravimetric analysis data, it can be argued that the thermal stability of the sulfated sample is lower than that of the original one. This is evidenced by the lower temperature of the onset of the main decomposition (250 °C for GA and 200 °C for GA-S), greater weight loss during the main stage of thermolysis (48.5% for GA and 62.6% for GA-S), as well as lower carbonized residue at the end of thermolysis (20.5%), while for the original sample this value was 26.5%. One of the likely reasons for the decrease in thermal stability of the sulfated sample is that the sulfuric acid formed at the initial stage of the main decomposition period further promoted the decomposition or depolymerization of gum arabic by removing some hydroxyl groups either through direct catalysis or through esterification mechanisms.[62]

A quantitative assessment of the thermal stability of substances can provide the determination of the apparent activation energy for the main stage of decomposition of a substance.[59,61] The activation energies of the samples were calculated by the Coates-Redfern integral method.[63] The calculated values of the main expansion are given in Table 2. The activation energy of the main stage of decomposition of sulfated GA is significantly lower (49.5 kJ/mol) than that of the original GA sample (86.5 kJ/mol), which confirms the lower thermal stability of GA-S. It can be assumed that the inclusion of sulfate groups in the structure of a substance has a catalytic effect on its thermal destruction.[61] In addition, during the sulfation process, hydroxyl groups are likely replaced by sulfate groups, which leads to a decrease in activation energy.[64]

Molecular geometry

Molecular geometry plays a crucial role in determining the physical and chemical properties of molecules. By studying the bond lengths and angles of GA 1, GA 2, and GA 3, we can gain insights into their stability, shape, and intermolecular interactions.[65] The geometric structures of GA 1, GA 2 and GA 3 molecules were optimized in the B3LYP/6-31G(d,p) basis set. The geometric parameters (bond lengths and angles) calculated in the gas phase of the compounds are presented in Table 3. The symmetry of GA 1, GA 2, and GA 3 molecules is C1 point group, which means they have a certain arrangement of atoms. The total energies of the molecules are -1186.811546, -1867.194832, and -2547.589060 Hartree, respectively. These values indicate the stability or energy state of the molecules. C-O bond lengths in compounds are in the range of 1.39-1.45 Å, and C-C bond lengths are in the range of 1.53-1.55 Å. The S-O bond lengths in GA 2 and GA 3 compounds are from 1.45 to 1.67 Å.

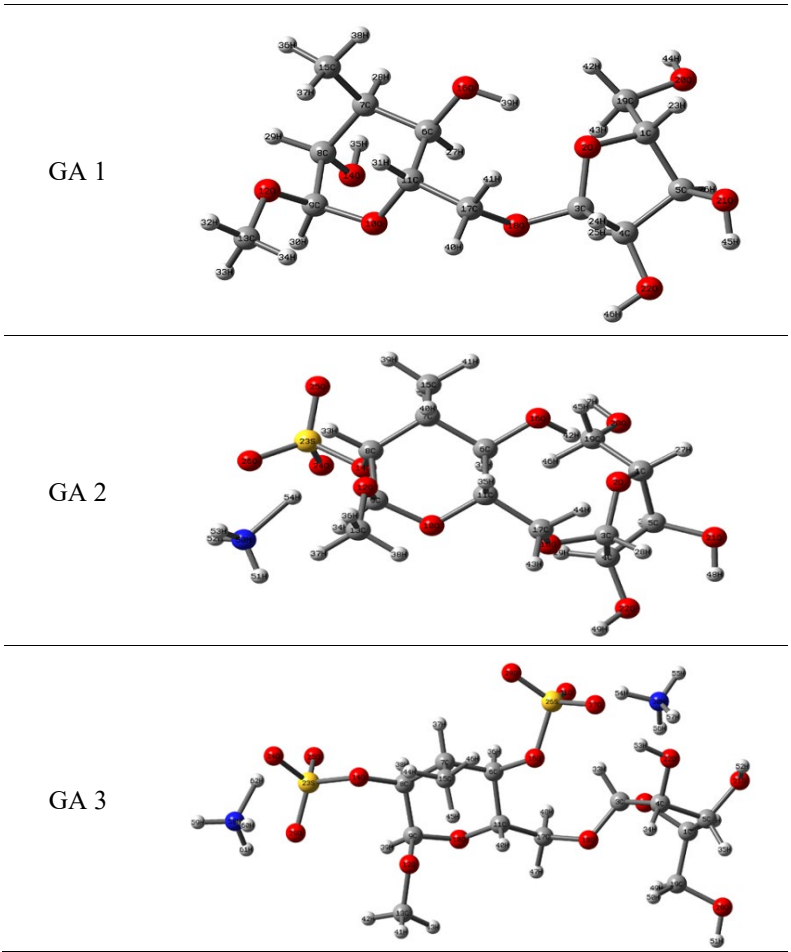

Figure 5: Optimized molecular geometry of gum arabic and gum arabic sulfates, along with their numbering of atoms

Table 3
Selected important bond parameters for gum arabic and gum arabic sulfates

Bond lengths (Å)					
GA 1		GA 2		GA 3	
Bonds	Values	Bonds	Values	Bonds	Values
C1-O2	1.4491	C1-O2	1.4499	C1-O2	1.4439
C1-C5	1.5332	C1-C5	1.5314	C1-C5	1.5329
O2-C3	1.4368	O2-C3	R(2.3)	O2-C3	1.4353
C3-C4	1.5307	C3-C4	R(3.4)	C3-C4	1.5483
C3-O18	1.3894	C3-O18	1.3929	C3-O18	1.3987
C4-C5	1.5319	C4-C5	1.5315	C4-C5	1.5669
C5-O21	1.4180	C5-O21	1.4181	C5-O21	1.4223
C4-O22	1.4148	C4-O22	1.4159	C4-O22	1.4242
C6-C7	1.5381	C6-C7	1.5392	C6-C7	1.5497
C6-C11	1.5387	C6-C11	1.5394	C6-C11	1.5409
C6-O16	1.4185	C6-O16	1.4177	C6-O16	1.4433
C7-C8	1.5442	C7-C8	1.5360	C7-C8	1.5379
C8-C9	1.5389	C8-C9	1.5375	C8-C9	1.5355
C8-O14	1.4290	C8-O14	1.4680	C8-O14	1.4500
C9-O10	1.4118	C9-O10	1.4094	C9-O10	1.4222
C9-O12	1.4104	C9-O12	1.4081	C9-O12	1.3967
O10-C11	1.4361	O10-C11	1.4406	O10-C11	1.4379
C11-C17	1.5224	C11-C17	1.5226	C11-C17	1.5362
O12-C13	1.4210	O12-C13	1.4221	O12-C13	1.4236

C17-O18	1.4380	C17-O18	1.4364	C17-O18	1.4319
C19-O20	1.4195	C19-O20	1.4196	C19-O20	1.4225
		O14-S23	1.6327	O14-S23	1.6380
		S23-O24	1.5696	S23-O24	1.5669
		S23-O25	1.4528	S23-O25	1.4532
		S23-O26	1.4679	S23-O29	1.4686
		N50-H51	1.0165	O16-S26	1.6718
		N50-H52	1.0166	S26-O27	1.4847
		N50-H53	1.0197	S26-O28	1.4584
		N50-H54	1.5460	S26-O30	1.5111
				N53-H54	1.0165
				N53-H55	1.0166
				N53-H56	1.0194
				N53-H57	1.5402
				N58-H59	1.0459
				N58-H60	1.0175
				N58-H61	1.0284
				N58-H62	1.0768
Bond angles (º)					
C1-O2-C3	110.7273	C1-O2-C3	110.9936	C1-O2-C3	107.8722
C1-C5-C4	102.1863	C1-C5-C4	102.0959	C1-C5-C4	103.8539
O2-C3-O18	111.4889	O2-C3-O18	111.933	O2-C3-O18	112.7526
C3-O18-C17	115.6839	C3-O18-C17	116.0717	C3-O18-C17	114.7559
C5-C1-C19	114.6072	C5-C1-C19	114.7825	C5-C1-C19	114.3099
C6-C7-C8	108.9771	C6-C7-C8	108.6557	C6-C7-C8	106.9315
C6-C7-C15	113.7105	C6-C7-C15	113.7319	C6-C7-C15	113.4754
C6-C11-O10	109.569	C6-C11-O10	109.8558	C6-C11-O10	108.6247
C9-O10-C11	114.7357	C9-O10-C11	114.6303	C9-O10-C11	115.5705
O10-C9-O12	112.4315	O10-C9-O12	112.8367	O10-C9-O12	112.8533
C11-C17-O18	111.2163	C11-C17-O18	111.3126	C11-C17-O18	113.1581
		C8-O14-S23	115.41	C6-O16-S26	118.4466
		O14-S23-O24	97.9	O16-S26-O27	99.7849
		O14-S23-O25	109.1191	O16-S26-O28	108262
		O14-S23-O26	107.9268	O16-S26-O30	103.7989
		H51-N50-H52	108.1479	C8-O14-S23	117.0747
		H51-N50-H53	108.4517	O14-S23-O24	98.0988
		H51-N50-H54	116.5213	O14-S23-O25	108.8334
				O14-S23-O29	108.2757
				H54-N53-H55	108.2533
				H54-N53-H56	108.4968
				H54-N53-H57	115.7042
				H59-N58-H60	112.1767
				H59-N58-H61	104.9304
				H59-N58-H62	105.9589

Frontier molecular orbital (FMO) analysis

The analysis of frontier molecular orbitals (FMOs) provides valuable information about the reactivity and stability of molecules.[66] By examining the HOMO and LUMO orbitals of GA 1, GA 2, and GA 3, we can gain insights into their chemical reactivity, biological activity, and kinetic stability. The HOMO represents the highest occupied energy level, while the LUMO represents the lowest unoccupied energy level. The energy gap between these two orbitals determines the reactivity of the molecule, with a smaller energy gap indicating higher reactivity. In the case of GA 1, GA 2, and GA 3, the order of energy gaps is GA 1> GA 3> GA 2, indicating that GA 2 is the most reactive molecule among them (Fig. 6).

Quantum chemical parameters, such as chemical potential, electron affinity, ionization potential, optical softness, chemical softness, chemical hardness, electronegativity, nucleophilicity index, electrophilicity index, and maximum charge transfer, provide valuable insights into the properties and behavior of molecules:[67,68]

$\mu = (E_{HOMO} + E_{LUMO})/2$ (2)
$EA = - E_{LUMO}$ (3)
$IP = -E_{HOMO}$ (4)
$\sigma_{\circ} = 1/2\eta$ (5)
$\zeta = 1/\eta$ (6)
$\eta = (E_{HOMO} - E_{LUMO})/2$ (7)
$\chi = -(E_{HOMO} + E_{LUMO})/2$ (8)
$N = -\mu/\eta$ (9)
$\omega = \mu^2/2\eta$ (10)
$\Delta N_{max} = (E_{HOMO} + E_{LUMO})/2(E_{HOMO} - E_{LUMO})$ (11)

These parameters are determined based on the HOMO and LUMO energies and can help us understand various aspects of the molecules' reactivity, stability, and interaction with other biomolecules. For example, a large energy gap or hardness value indicates a hard molecule, while a small energy gap or softness value indicates a soft molecule. The electrophilic index value and the maximum charge transfer index provide information about the molecule's ability to bind to biomolecules. Analyzing these quantum chemical parameters allows us to gain a deeper understanding of the molecular properties and potential applications.

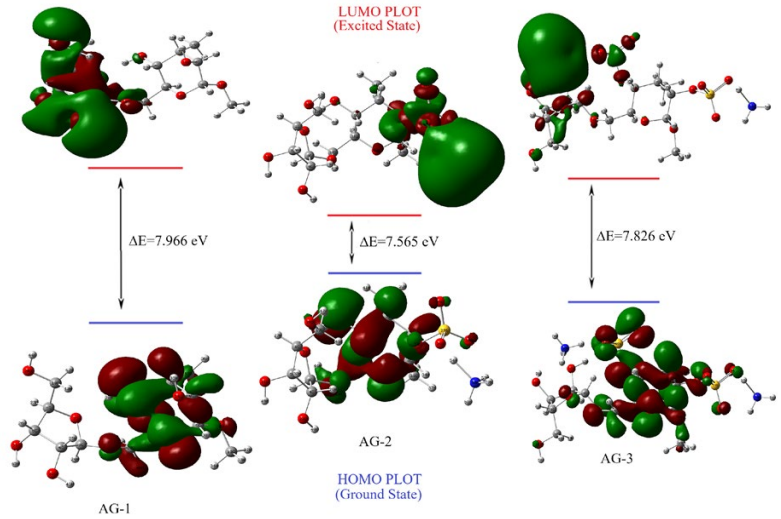

Figure 6: Calculated HOMO and LUMO orbitals, and the energy gap plots of gum arabic and gum arabic sulfates by B3LYP/6-31g(d,p)

Table 4
Selected important reactivity descriptors for gum arabic and gum arabic sulfates

Parameters	Values (eV)		
	GA 1	GA 2	GA 3
E_{LUMO} (Energy of LUMO)	1.4199	0.9927	0.8675
E_{HOMO} (Energy of HOMO	-6.5468	-6.5724	-6.9593
ΔE (Energy gap)	7.9667	7.5650	7.8268
μ (Chemical potential)	-2.5634	-2.7898	-3.0459
EA (Electron affinity)	-1.4199	-0.9927	-0.8675
IP (Ionization potential)	6.5468	6.5724	6.9593
$\sigma_{\circ}$ (Optical softness)	0.1255	0.1322	0.1278
ζ (Chemical softness)	0.2510	0.2644	0.2555
η (Chemical hardness)	3.9833	3.7825	3.9134
χ (Electronegativity)	2.5634	2.7898	3.0459
N (Nucleophilicity index)	1.2123	0.9720	0.8436
ω (Electrophilicity index)	0.8248	1.0288	1.1854
ΔN_{max} (Maximum charge transfer index)	0.6435	0.7376	0.7783

The calculated quantum chemical parameters provide valuable insights into the electronic structure and properties of the molecules. For example, the chemical potential (μ) is the average of the HOMO and LUMO energies and represents the ability of the molecule to donate or accept electrons. Table 4 shows some important quantum chemical parameters calculated for GA 1, GA 2,

and GA 3 molecules. A large energy gap or a large hardness value indicates a hard molecule, while a small energy gap or a large softness value indicates a soft molecule. In this case, we can say that the softest molecule is AG2, and the hardest molecule is GA 1. A higher chemical potential indicates a more reactive molecule.[69] The electrophilic index measures the ability of the molecule to act as an electrophile, with values above 1.5 eV indicating a strong electrophile.[70] The maximum charge transfer index provides information about the molecule's ability to bind to biomolecules. In this study, GA 3 has the highest electrophilic index and maximum charge transfer index, suggesting its strong binding ability to biomolecules.

Molecular electrostatic potential (MEP) surface analysis

The molecular electrostatic potential (MEP) surface analysis provides valuable insights into the size, shape, delocalization, and chemical reactivity of molecules.[71] By visualizing the MEP surface, we can identify the regions of positive and negative electrostatic potential, as well as the areas of near-zero potential. This information helps us understand the electrophilic and nucleophilic active regions of the molecules, which are crucial for predicting intermolecular interactions and hydrogen bonding. By analyzing the MEP surface of GA 1, GA 2, and GA 3, we can gain a better understanding of their chemical reactivity and potential for interaction with other molecules. Figure 7 depicts the MEP surface calculated at the DFT: B3LYP/6-31G(d,p) level of theory of molecules GA 1, GA 2, and GA 3. The values of the electrostatic potentials are represented by different colors, and the potential increases in the order of red < orange < yellow < green < blue. The blue surface on the MEP map covers the positive electrostatic potential region, and the red surface covers the negative electrostatic potential region. The green colored surface represents the region of near zero electrostatic potential. The electron density on the surface of the molecule changed in the following order: GA 1 (0.059 a.u.) < GA 2 (0.062 a.u.) < GA 3 (0.083 a.u.) on the positive side, and vice versa on the negative side.

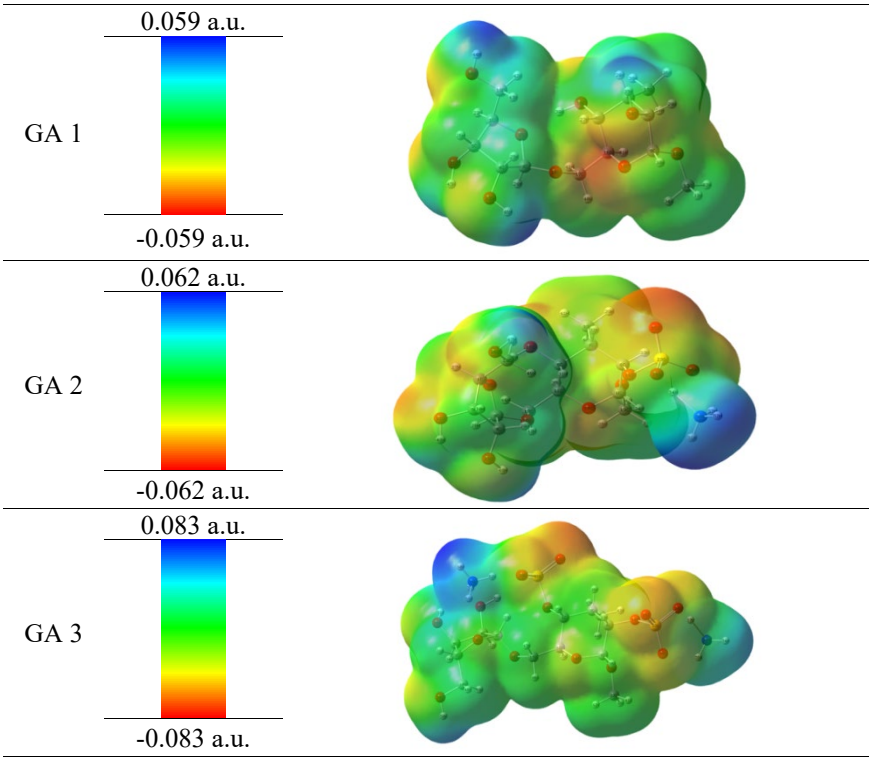

Figure 7: Molecular electrostatic potential maps for gum arabic and gum arabic sulfates with color code

Vibrational analysis

Vibrational spectroscopy is a powerful tool for identifying and confirming the functional groups present in organic molecules.[72] By studying the vibrational frequencies of GA 1, GA 2, and GA 3, we can gain insights into the types of bonds and motions present in these molecules. For example, the O-H stretching frequency provides information

about the presence of hydroxyl groups, while the C-H stretching frequencies indicate the presence of carbon-hydrogen bonds. Similarly, the N-H stretching and bending frequencies reveal the characteristics of the N-H group and its interactions within the molecules. Understanding the vibrational properties of GA 1, GA 2, and GA 3 allows us to further characterize these molecules and predict their behavior in various chemical reactions. GA 1, GA 2, and GA 3 molecules consist of 46, 54, and 62 atoms, respectively, with 132, 156, and 180 normal vibrational modes, respectively. Calculated and experimental vibrational frequencies (scaled) are listed in Table 5. The calculated frequencies are scaled using a scaling factor of 0.9608. The simulated FT-IR spectra of the molecules are shown in Figure 8.

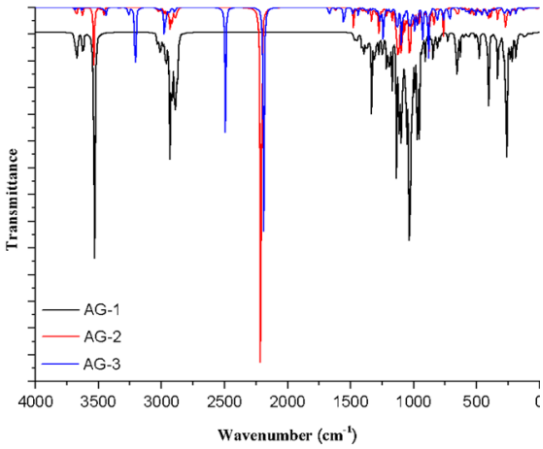

Figure 8: Calculated FT-IR spectra for gum arabic and gum arabic sulfates

Table 5
Selected important vibrational frequencies (cm^{-1}) determined theoretically (scaled by a factor of 0.9608) and experimentally for gum arabic and gum arabic sulfates

GA 1		GA 2		GA 3	
Assignments	Theo.	Assignments	Theo.	Assignments	Theo.
υO-H	3683-3530	υO-H	3681-3533	υO-H	3684, 3631, 3207
υC-H	3031-2868	υN-H	3477, 3455, 3334, 2210	υN-H	3478-3260, 2493, 2188
υC-O-C connecting two rings)	1131	υC-H	3033-2875	υC-H	3046-2892
$\upsilon O\text{-}CH_3$	1113	υC-O-C connecting two rings)	1127	υC-O-C (connecting two rings)	1093
$\upsilon HO\text{-}CH_2$	1034	$\upsilon O\text{-}CH_3$	1092	$\upsilon O\text{-}CH_3$	1083
		$\upsilon HO\text{-}CH_2$	1053	$\upsilon HO\text{-}CH_2$	1042
		δN-H	1621, 1610, 1475, 1138, 1122, 1100	δN-H	1674-1552, 15481, 1439, 1359, 1272, 1137, 1125, 1097
		υS-O	1276, 1100, 9879, 763	υS-O	1272, 1145, 1098, 1097, 927, 882, 760, 714

O-H vibrations

The O-H stretching frequency is determined in a wide bandgap range from 3690 to 3100 cm^{-1}.[73] Vibrations of the free hydroxyl group appear in the region 3700–3584 cm^{-1}.[74]

C-H vibrations

C-H stretching frequencies typically range from 3100 to 3000 cm^{-1} [75] and occur as a broad band. In this study, the calculated C-H vibrations of GA 1, GA 2 and GA 3 molecules occur in the regions

between 3031-2868 cm^{-1}, 3033-2875 cm^{-1} and 3046-2892 cm^{-1}, respectively.

N-H vibrations

It is known[76] that the N-H stretching vibration frequencies lie in the range of 3300-3500 cm^{-1}. In this study, the calculated vibration frequencies of the N-H group in the N…H…O hydrogen bridge in the molecules are 2210 (GA 2), 2188 and 2493 cm^{-1} (GA 3), respectively. NH symmetric stretching frequency of GA 2 molecule is 3334 cm^{-1}, NH asymmetric stretching frequencies are 3455 and 3477 cm^{-1}. NH stretching frequencies for the GA 3 molecule are in the range of 3478-3260 cm^{-1}. The calculated N-H bending frequencies range from 1621 to 1100 cm^{-1} for the GA 2 molecule and from 1674 to 1097 cm^{-1} for the GA 3 molecule.

Fukui functions

The calculated Fukui functions are valuable reactivity indices that can provide insights into the preferred sites of electrophilic and nucleophilic attacks in molecules.[77] By determining the atoms with the maximum value of Fukui function and local softness, scientists can predict the regions where a molecular chemical species is likely to alter its electron density. These predictions can be crucial in understanding the behavior and reactivity of molecules, as well as in designing and optimizing chemical reactions.

For example, knowing the preferred sites of electrophilic and nucleophilic attacks can aid in the development of more efficient and selective catalysts.

The Fukui functions of j_{th} atom site are defined as follows:[78]

$$f_j^- = q_j(N) - q_j(N-1) \quad (12)$$

$$f_j^+ = q_j(N+1) - q_j(N) \quad (13)$$

$$f_j^0 = \left[q_j(N+1) - q_j(N-1)\right]/2 \quad (14)$$

where electrophilic, nucleophilic, or free radical attacks on the reference molecule are represented by $f^-_j(r)$, $f^+_j(r)$, respectively. In these equations, q_j represents the atomic charge at the j_{th} atomic site in the neutral (N), anionic (N+1), or cationic (N-1) chemical species. The equation gives a dual descriptor (f(r)), which is defined as the difference between the nucleophilic and electrophilic Fukui functions:

$$\Delta f(r) = f^+(r) - f^-(r) \quad (15)$$

where $f^+(r)$ indicates the nucleophilic reactivity of an atom (atoms with high f^+ values are more likely to undergo nucleophilic attacks); $f^-(r)$ indicates the electrophilic reactivity of an atom (atoms with high $f^-(r)$ values are more prone to accept electrons, making them electrophilic); $f^0(r)$ represents the overall reactivity of an atom and is the sum of $f^+(r)$ and $f^-(r)$. Dual descriptor f(r) distinguishes between nucleophilic and electrophilic attacks at a certain site based on their signs.

Fukui functions and dual descriptors for title compounds were calculated using the Multiwfn[25] software and are listed in Table 6. The highest reactivity order for the nucleophile and electrophile of atoms in GA 1 is H46 > H44 and O16 > O10 > O21, respectively. The highest reactivity order for the nucleophile and electrophile of atoms in GA 2 is H52 > H49 > H51 > H53 > H47 and O16 > O10 > O21, respectively. The highest reactivity order for the nucleophile and electrophile of atoms in GA 3 is H60 > H54 > H55 > H58 > H61 > H56 and O10 > O20 > O16, respectively.

CONCLUSION

The possibility of sulfating gum arabic with sulfamic acid in 1,4-dioxane in the presence of urea has been shown. It has been established that the sulfuric acid esters obtained in this way have higher sulfur content than when using a similar method for arabinogalactan. The introduction of a sulfate group into the gum arabic molecule is proven by the appearance of absorption bands at 1249 cm^{-1}. According to NMR data, a new signal appears in the 13C NMR spectrum at 52.3 ppm, which may correspond to the C1 or C6 atoms of sulfated gum. The new peak arrangement probably reflects sulfation at C2, C3, or C4 sugar units, particularly galactose or glucuronic acid residues. Using thermal analysis, it was established that the introduction of a sulfate group into a biopolymer macromolecule leads to a decrease in its thermal stability and a decrease in activation energy from 86.5 to 49.5 kJ/mol.

The DFT method was used to calculate the original gum arabic and its sulfated derivatives. For the calculations, the dimer was taken as reflecting the structure of the polymer. The structure was optimized, HOMO-LUMO, FMO, MEP and Fukui functions were calculated.

Table 6
Fukui functions and dual descriptor for gum arabic and gum arabic sulfates

	GA 1					GA 2					GA 3			
Atoms	f_r^-	f_r^+	f_r^0	Δf(r)	Atoms	f_r^-	f_r^+	f_r^0	Δf(r)	Atoms	f_r^-	f_r^+	f_r^0	Δf(r)
1(C)	0.0059	0.023	0.0144	0.0171	1(C)	0.0051	0.0134	0.0093	0.0083	1(C)	0.0047	0.0068	0.0058	0.0021
2(O)	0.0069	0.0212	0.0141	0.0143	2(O)	0.0038	0.0121	0.008	0.0084	2(O)	0.0126	0.0055	0.0091	-0.0072
3(C)	0.0092	0.0168	0.013	0.0075	3(C)	0.0078	0.01	0.0089	0.0022	3(C)	0.0025	0.0017	0.0021	-9E-4
4(C)	0.0097	0.0256	0.0176	0.0159	4(C)	0.0084	0.0166	0.0125	0.0082	4(C)	0.0026	0.0037	0.0031	0.0011
5(C)	0.015	0.015	0.015	0	5(C)	0.0142	0.01	0.0121	-0.0042	5(C)	0.0063	0.0055	0.0059	-8E-4
6(C)	0.0315	0.0017	0.0166	-0.0299	6(C)	0.0307	5E-4	0.0156	-0.0302	6(C)	0.0157	0.0046	0.0101	-0.0111
7(C)	0.0098	0.0087	0.0093	-0.001	7(C)	0.0108	0.002	0.0064	-0.0087	7(C)	0.0155	0.002	0.0088	-0.0135
8(C)	0.0152	0.0128	0.014	-0.0024	8(C)	0.0113	0.0138	0.0125	0.0025	8(C)	0.0134	0.0068	0.0101	-0.0065
9(C)	0.0144	0.0069	0.0107	-0.0075	9(C)	0.0137	0.0035	0.0086	-0.0102	9(C)	0.0176	0.0026	0.0101	-0.015
10(O)	0.0939	0.0027	0.0483	-0.0912	10(O)	0.0831	0.0012	0.0422	-0.0819	10(O)	0.0664	0.0075	0.037	-0.0589
11(C)	0.0312	0.0034	0.0173	-0.0278	11(C)	0.032	0.0018	0.0169	-0.0302	11(C)	0.0192	0.0032	0.0112	-0.016
12(O)	0.0251	0.0059	0.0155	-0.0193	12(O)	0.0125	0.0058	0.0091	-0.0067	12(O)	0.0094	-0.001	0.0042	-0.0104
13(C)	0.0112	0.0089	0.0101	-0.0023	13(C)	0.0095	0.0072	0.0084	-0.0023	13(C)	0.0096	0.0033	0.0065	-0.0063
14(O)	0.0179	0.0348	0.0263	0.0169	14(O)	0.0092	0.0203	0.0147	0.0111	14(O)	0.0317	0.0127	0.0222	-0.0191
15(C)	0.0101	0.0086	0.0093	-0.0015	15(C)	0.0094	0.0066	0.008	-0.0028	15(C)	0.0096	0.0035	0.0065	-0.0061
16(O)	0.1157	0.0101	0.0629	-0.1056	16(O)	0.1145	0.0107	0.0626	-0.1038	16(O)	0.0411	0.0079	0.0245	-0.0332
17(C)	0.0109	0.0087	0.0098	-0.0022	17(C)	0.011	0.0052	0.0081	-0.0058	17(C)	0.0103	0.0028	0.0065	-0.0075
18(O)	0.0161	0.0058	0.011	-0.0104	18(O)	0.0157	8E-4	0.0082	-0.0149	18(O)	0.0314	0.0058	0.0186	-0.0256
19(C)	0.0059	0.023	0.0144	0.0171	19(C)	0.0051	0.0093	0.0072	0.0042	19(C)	0.0113	0.0139	0.0126	0.0026
20(O)	0.0297	0.0507	0.0402	0.021	20(O)	0.0295	0.0231	0.0263	-0.0064	20(O)	0.0505	0.0227	0.0366	-0.0279
21(O)	0.0695	0.0294	0.0494	-0.0401	21(O)	0.0658	0.0212	0.0435	-0.0446	21(O)	0.0243	0.0099	0.0171	-0.0144
22(O)	0.0239	0.0633	0.0436	0.0394	22(O)	0.021	0.0431	0.0321	0.0221	22(O)	0.0127	0.0081	0.0104	-0.0046
23(H)	0.0136	0.0241	0.0188	0.0105	23(S)	0.0121	0.0398	0.0259	0.0277	23(S)	0.0133	0.0247	0.019	0.0114
24(H)	0.0197	0.0175	0.0186	-0.0022	24(O)	0.0132	0.0252	0.0192	0.012	24(O)	0.0228	0.0202	0.0215	-0.0026
25(H)	0.0088	0.0193	0.014	0.0105	25(O)	0.0305	0.045	0.0377	0.0144	25(O)	0.0293	0.0291	0.0292	-2E-4
26(H)	0.0268	0.0153	0.021	-0.0114	26(O)	0.0346	0.0313	0.033	-0.0033	26(S)	0.0245	0.0143	0.0194	-0.0103
27(H)	0.0255	2E-4	0.0129	-0.0253	27(H)	0.0126	0.0163	0.0144	0.0038	27(O)	0.0439	0.0118	0.0278	-0.032
28(H)	0.0274	0.0202	0.0238	-0.0072	28(H)	0.018	0.0122	0.0151	-0.0059	28(O)	0.0657	0.022	0.0439	-0.0436
29(H)	0.0303	0.0206	0.0255	-0.0097	29(H)	0.0074	0.011	0.0092	0.0037	29(O)	0.0328	0.0194	0.0261	-0.0134
30(H)	0.0233	0.0093	0.0163	-0.014	30(H)	0.0248	0.0102	0.0175	-0.0147	30(O)	0.0344	0.0061	0.0202	-0.0283
31(H)	0.0301	0.0113	0.0207	-0.0189	31(H)	0.0245	-0.0035	0.0105	-0.028	31(H)	0.013	0.009	0.011	-0.004
32(H)	0.018	0.011	0.0145	-0.0069	32(H)	0.025	0.0023	0.0136	-0.0227	32(H)	3E-4	-1E-4	1E-4	-5E-4
33(H)	0.0166	0.01	0.0133	-0.0065	33(H)	0.0195	0.0151	0.0173	-0.0044	33(H)	0.0065	0.0099	0.0082	0.0034
34(H)	0.0064	0.0033	0.0048	-0.0032	34(H)	0.0195	5E-4	0.01	-0.019	34(H)	0.0119	0.0109	0.0114	-0.001
35(H)	0.015	0.0903	0.0526	0.0753	35(H)	0.0292	0.0081	0.0186	-0.0211	35(H)	0.0122	0.0041	0.0082	-0.0082
36(H)	0.0216	0.0132	0.0174	-0.0083	36(H)	0.0161	0.0105	0.0133	-0.0056	36(H)	0.0256	0.0034	0.0145	-0.0222

37(H)	0.0098	0.0088	0.0093	-9E-4	37(H)	0.0135	0.0046	0.009	-0.0088	37(H)	0.013	0.0063	0.0097	-0.0067
38(H)	0.0103	0.0078	0.009	-0.0025	38(H)	0.0042	0.0046	0.0044	4E-4	38(H)	0.0178	0.0053	0.0116	-0.0125
39(H)	0.0239	0.004	0.0139	-0.0199	39(H)	0.0196	0.0069	0.0133	-0.0127	39(H)	0.017	0.0047	0.0109	-0.0122
40(H)	0.0238	0.0147	0.0193	-0.0092	40(H)	0.0108	0.0061	0.0084	-0.0047	40(H)	0.0142	0.0052	0.0097	-0.009
41(H)	0.0138	0.0126	0.0132	-0.0012	41(H)	0.0099	0.0099	0.0099	0	41(H)	0.0114	0.0032	0.0073	-0.0082
42(H)	0.0051	0.0188	0.012	0.0137	42(H)	0.0238	0.0049	0.0144	-0.0188	42(H)	0.0061	0.0046	0.0054	-0.0015
43(H)	0.0034	0.012	0.0077	0.0086	43(H)	0.0237	0.0085	0.0161	-0.0152	43(H)	0.0151	0.0046	0.0098	-0.0105
44(H)	0.0158	0.1078	0.0618	0.0921	44(H)	0.0133	0.0097	0.0115	-0.0036	44(H)	0.0121	0.0034	0.0078	-0.0087
45(H)	0.0208	0.0283	0.0245	0.0075	45(H)	0.0041	0.0087	0.0064	0.0046	45(H)	0.0094	0.0051	0.0073	-0.0043
46(H)	0.0117	0.1327	0.0722	0.121	46(H)	0.0023	0.0014	0.0019	-9E-4	46(H)	0.0185	0.0072	0.0129	-0.0113
					47(H)	0.0146	0.0425	0.0285	0.0279	47(H)	0.0108	0.0018	0.0063	-0.009
					48(H)	0.0199	0.0189	0.0194	-0.001	48(H)	0.0147	0.0115	0.0131	-0.0032
					49(H)	0.0108	0.0904	0.0506	0.0796	49(H)	0.0097	0.0101	0.0099	4E-4
					50(N)	0.0025	0.061	0.0317	0.0586	50(H)	0.0185	0.0451	0.0318	0.0266
					51(H)	0.0036	0.0897	0.0466	0.0861	51(H)	0.0099	0.0185	0.0142	0.0086
					52(H)	0.0088	0.0939	0.0513	0.0851	52(H)	0.0033	0.0057	0.0045	0.0024
					53(H)	0.0012	0.0583	0.0298	0.0571	53(N)	0.0028	0.047	0.0249	0.0442
					54(H)	0.0028	0.0179	0.0104	0.0151	54(H)	0.0089	0.0732	0.0411	0.0643
										55(H)	0.0041	0.0683	0.0362	0.0642
										56(H)	0	0.0437	0.0219	0.0437
										57(H)	0.004	0.0134	0.0087	0.0094
										58(N)	0.0057	0.0574	0.0315	0.0517
										59(H)	0.0014	0.0241	0.0128	0.0227
										60(H)	0.0112	0.1377	0.0744	0.1266
										61(H)	0.0033	0.0471	0.0252	0.0438
										62(H)	0.0023	0.0217	0.012	0.0194

The obtained results are a continuation of systematic work on the study of the sulfamic acid-urea mixture as a sulfating agent. This mixture has a number of advantages over traditional sulfation methods and we hope that our studies will lead to the development of more environmentally friendly and safe methods for obtaining polysaccharide sulfates.

ACKNOWLEDGMENTS: The authors thank the University of Bingöl for providing the server and the University of Bitlis Eren for providing the Gaussian 09W software. Experimental work was conducted within the framework of the budget plan # 0287-2021-0017 for Institute of Chemistry and Chemical Technology SB RAS using the equipment of Krasnoyarsk Regional Research Equipment Center of SB RAS. Theoretical work was supported Researchers Supporting Project number (RSP2024R61), King Saud University, Riyadh, Saudi Arabia.

REFERENCES

[1] T. Mahendran, P. A. Williams, G. O. Phillips, S. Al-Assaf and T. C. Baldwin, *J. Agric. Food Chem.*, **56**, 9269 (2008), https://doi.org/10.1021/jf800849a

[2] S.-P. Nie, C. Wang, S. W. Cui, Q. Wang, M.-Y. Xie *et al.*, *Food Hydrocol.*, **31**, 42 (2013), https://doi.org/10.1016/j.foodhyd.2012.09.014

[3] H. H. Musa, A. A. Ahmed and T. H. Musa, in "Bioactive Molecules in Food", edited by J.-M. Mérillon and K. G. Ramawat, Springer International Publishing, Cham, 2017, pp. 1-18

[4] N. E. Siddig, M. E. Osman, S. Al-Assaf, G. O. Phillips and P. A. Williams, *Food Hydrocol.*, **19**, 679 (2005), https://doi.org/10.1016/j.foodhyd.2004.09.005

[5] S. S. Banerjee and D.-H. Chen, *J. Hazard. Mater.*, **147**, 792 (2007), https://doi.org/10.1016/j.jhazmat.2007.01.079

[6] S. A. Mohamed, A. M. Elsherbini, H. R. Alrefaey, K. Adelrahman, A. Moustafa *et al.*, *Nanomaterials*, **15**, 290 (2025), https://doi.org/10.3390/nano15040290

[7] M. E. Vuillemin, F. Michaux, A. A. Adam, M. Linder, L. Muniglia *et al.*, *Food Hydrocol.*, **107**, 105919 (2020), https://doi.org/10.1016/j.foodhyd.2020.105919

[8] P. Brzyski, *Materials*, **14**, 6775 (2021), https://doi.org/10.3390/ma14226775

[9] A. H. Pandit, N. Mazumdar, K. Imtiyaz, M. M. A. Rizvi and S. Ahmad, *ACS Omega*, **4**, 16026 (2019), https://doi.org/10.1021/acsomega.9b02137

[10] F. W. M. Ribeiro, L. de S. Laurentino, C. R. Alves, M. de S. R. Bastos, J. M. C. de Costa *et al.*, *J. Appl. Polym. Sci.*, **132**, (2015), https://doi.org/10.1002/app.41519

[11] S. Mohamed and D. R. Coombe, *Pharmaceuticals*, **10**, 78 (2017), https://doi.org/10.3390/ph10040078

[12] H. E. Caputo, J. E. Straub and M. W. Grinstaff, *Chem. Soc. Rev.*, **48**, 2338 (2019), https://doi.org/10.1039/c7cs00593h

[13] M. A. Torlopov and S. V. Frolova, *Chem. Plant Raw Mater.*, **3**, 63 (2007)

[14] M. A. Torlopov, S. V. Frolova and V. A. Demin, *Chem. Sust. Develop.*, **15**, 483 (2007)

[15] Z. M. Wang, L. Li, B. S. Zheng and N. Normakhamatov, *Int. J. Biol. Macromol.*, **41**, 376 (2007), https://doi.org/10.1016/j.ijbiomac.2007.05.007

[16] Z.-M. Wang, L. Li, K.-J. Xiao and J.-Y. Wu, *Bioresour. Technol.*, **100**, 1687 (2009), https://doi.org/10.1016/j.biortech.2008.09.002

[17] M. Gericke, T. Liebert and T. Heinze, *Macromol. Biosci.*, **9**, 343 (2009), https://doi.org/10.1002/mabi.200800329.

[18] W. Wagenknecht, I. Nehls, J. Kotz and B. Philipp, *Cellulose Chem. Technol.*, **25**, 343 (1993), https://www.cellulosechemtechnol.ro/

[19] W. Wagenknecht and I. Nehls, *Carbohyd. Res.*, **240**, 245 (1993)

[20] X. Huang and W.-D. Zhang, *J. Fiber Bioeng. Inform.*, **3**, 32 (2010), https://doi.org/10.3993/jfbi06201006

[21] R. A. Al-Horani and U. R. Desai, *Tetrahedron*, **66**, 2907 (2010), https://doi.org/10.1016/j.tet.2010.02.015

[22] J. A. Sirviö, J. Ukkola and H. Liimatainen, *Cellulose*, **26**, 2303 (2019), https://doi.org/10.1007/s10570-019-02257-8

[23] M. J. Frisch, G. W. Trucks, H. B. Schlegel, G. E. Scuseria, M. A. Robb *et al.*, Gaussian, Inc., Wallingford CT, 2009

[24] Gaussian, Inc., Semichem. Inc., Carnergie Office Parck-Building 6, Pittsburgh PA, 2000-2003

[25] T. Lu and F. Chen, *J. Comp. Chem.*, **33**, 580 (2012), https://doi.org/10.1002/jcc.22885

[26] D. Renard, L. Lavenant-Gourgeon, M.-C. Ralet and C. Sanchez, *Biomacromolecules*, **7**, 2637 (2006), https://doi.org/10.1021/bm060145j

[27] N. Y. Vasil'eva, A. V. Levdansky, B. N. Kuznetsov, G. P. Skvortsova, A. S. Kazachenko *et al.*, *Russ. J. Bioorg. Chem.*, **41**, 725 (2015), https://doi.org/10.1134/s1068162015070158

[28] A. S. Kazachenko, N. Y. Vasilieva, Y. D. Berezhnaya, O. Y. Fetisova, V. S. Borovkova *et al.*, *Polymers*, **15**, 1116 (2023), https://doi.org/10.3390/polym15051116

[29] A. V. Levdansky, N. Y. Vasilyeva, A. A. Kondrasenko, V. A. Levdansky, Y. N. Malyar *et al.*, *Wood Sci. Technol.*, **55**, 1725 (2021), https://doi.org/10.1007/s00226-021-01341-2

[30] A. S. Kazachenko, N. Y. Vasilieva, V. S. Borovkova, O. Y. Fetisova, N. Issaoui *et al.*, *Foods*, **10** (2021), https://doi.org/10.3390/foods10112571

[31] A. S. Kazachenko, Y. N. Malyar, N. Y. Vasilyeva, O. Y. Fetisova, A. I. Chudina *et al.*, *Wood Sci. Technol.*,

55, 1091 (2021), https://doi.org/10.1007/s00226-021-01299-1
[32] A. S. Kazachenko, Y. N. Malyar, N. Y. Vasilyeva, V. S. Borovkova and N. Issaoui, *Biomass Convers. Biorefin.*, (2021), https://doi.org/10.1007/s13399-021-01895-y
[33] R. A. Al-Horani and U. R. Desai, *Tetrahedron*, **66**, 2907 (2010), https://doi.org/10.1016/j.tet.2010.02.015
[34] E. E. Gilbert, *Chem. Rev.*, **62**, 549 (1962), https://doi.org/10.1021/cr60220a003
[35] W. Spillane and J.-B. Malaubier, *Chem. Rev.*, **114**, 2507 (2014), https://doi.org/10.1021/cr400230c
[36] A. S. Kazachenko, N. Y. Vasilieva, Y. N. Malyar, A. A. Karacharov, A. A. Kondrasenko *et al.*, *Biomass Convers. Biorefin.*, (2022), https://doi.org/10.1007/s13399-021-02250-x
[37] Y. N. Malyar, N. Y. Vasilyeva, A. S. Kazachenko, V. S. Borovkova, A. M. Skripnikov *et al.*, *Molecules*, **26**, 5364 (2021), https://doi.org/10.3390/molecules26175364
[38] J. Munoz-Munoz, D. Ndeh, P. Fernandez-Julia, G. Walton, B. Henrissat *et al.*, *mBio*, **12**, https://doi.org/10.1128/mbio.01368-01321
[39] W. Yao, Y. Weng and J. M. Catchmark, *Cellulose*, **27**, 5563 (2020), https://doi.org/10.1007/s10570-020-03177-8
[40] P. D. Carà, M. Pagliaro, A. Elmekawy, D. R. Brown, P. Verschuren *et al.*, *Catal. Sci. Technol.*, **3**, 2057 (2013), https://doi.org/10.1039/c3cy20838a
[41] A. S. Kazachenko, F. Akman, A. Sagaama, N. Issaoui, Y. N. Malyar, *et al.*, *J. Mol. Model.*, **27**, 5 (2021), https://doi.org/10.1007/s00894-020-04645-5
[42] D. Mudgil, S. Barak and B. S. Khatkar, *Int. J. Biol. Macromol.*, **50**, 1035 (2012), https://doi.org/10.1016/j.ijbiomac.2012.02.031
[43] A. S. Kazachenko, N. Y. Vasilyeva, F. Akman, O. Y. Fetisova, Y. D. Berezhnaya *et al.*, *J. Mol. Struct.*, **1294**, 136471 (2023), https://doi.org/10.1016/j.molstruc.2023.136471
[44] E. Atkins, in "Novel Biodegradable Microbial Polymers", edited by E. A. Dawes, Springer, Netherlands, Dordrecht, 1990, pp. 371-386
[45] I. Benalaya, G. Alves, J. Lopes and L. R. Silva, *Int. J. Mol. Sci.*, **25**, 1322 (2024), https://doi.org/10.3390/ijms25021322
[46] A. U. Elinwa and M. Umar, *Construct. Build. Mater.*, **156**, 632 (2017), https://doi.org/10.1016/j.conbuildmat.2017.08.162
[47] T. Şişmanoğlu, S. Karakuş, Ö. Birer, G. S. P. Soylu, A. Kolan *et al.*, *Appl. Surf. Sci.*, **354**, 250 (2015), https://doi.org/10.1016/j.apsusc.2015.07.206
[48] A. S. Kazachenko, F. Akman, Y. N. Malyar, N. Issaoui, N. Y. Vasilieva *et al.*, *J. Mol. Struct.*, **1245**, 131083 (2021), https://doi.org/10.1016/j.molstruc.2021.131083
[49] A. Kazachenko, F. Akman, M. Medimagh, N. Issaoui, N. Vasilieva *et al.*, *ACS Omega*, **6**, 22603 (2021), https://doi.org/10.1021/acsomega.1c02570
[50] K. H. M. Jonsson, E. Säwén and G. Widmalm, *Org. Biomol. Chem.*, **10**, 2453 (2012), https://doi.org/10.1039/c2ob06924e
[51] H.-X. Wang, J. Zhao, D.-M. Li, S. Song, L. Song *et al.*, *Carbohyd. Res.*, **402**, 95 (2015), https://doi.org/10.1016/j.carres.2014.10.010
[52] R. M. A. Daoub, A. H. Elmubarak, M. Misran, E. A. Hassan and M. E. Osman, *J. Saudi Soc. Agric. Sci.*, **17**, 241 (2018), https://doi.org/10.1016/j.jssas.2016.05.002
[53] E. I. Nep and B. R. Conway, *J. Excipients Food Chem.*, 1 (2010)
[54] D. M. W. Anderson, J. R. A. Millar and W. Weiping, *Food Addit. Contam.*, **8**, 405 (1991), https://doi.org/10.1080/02652039109373991
[55] L. Zhao, K. Ma and Z. Yang, *Int. J. Mol. Sci.*, **16**, 8454 (2015)
[56] E. Prokhorov, G. Luna-Barcenas, S. Kumar-Krishnan, R. A. Mauricio Sánchez, B. E. Castillo Reyes *et al.*, *J. Mol. Struct.*, **1218**, 128531 (2020), https://doi.org/10.1016/j.molstruc.2020.128531
[57] R. de Cássia Almeida Sampaio, R. S. da Costa, C. R. F. de Souza, A. P. Duarte Júnior, R. M. Ribeiro-Costa *et al.*, *J. Therm. Anal. Calorim.*, **123**, 2469 (2016), https://doi.org/10.1007/s10973-015-5123-x
[58] C. G. Mothé and M. A. Rao, *Thermochim. Acta*, **357-358**, 9 (2000), https://doi.org/10.1016/S0040-6031(00)00358-0
[59] M. J. Zohuriaan and F. Shokrolahi, *Polym. Test.*, **23**, 575 (2004), https://doi.org/10.1016/j.polymertesting.2003.11.001
[60] T. K. Q. Doan and K. Y. Chiang, *Sust. Environ. Res.*, **32**, 26 (2022), https://doi.org/10.1186/s42834-022-00136-9
[61] M. Roman and W. T. Winter, *Biomacromolecules*, **5**, 1671 (2004), https://doi.org/10.1021/bm034519+
[62] M. R. K. Sofla, R. J. Brown, T. Tsuzuki and T. J. Rainey, *Adv. Nat. Sci.: Nanosci. Nanotech.*, **7**, 035004 (2016), https://doi.org/10.1088/2043-6262/7/3/035004
[63] A. W. Coats and J. P. Redfern, *Nature*, **201**, 68 (1964), https://doi.org/10.1038/201068a0
[64] M. A. Henrique, W. P. Flauzino Neto, H. A. Silvério, D. F. Martins, L. V. A. Gurgel *et al.*, *Ind. Crop. Prod.*, **76**, 128 (2015), https://doi.org/10.1016/j.indcrop.2015.06.048
[65] A. S. Kazachenko, F. N. Tomilin, A. A. Pozdnyakova, N. Y. Vasilyeva, Y. N. Malyar *et al.*, *Chem. Pap.*, **74**, 4103 (2020), https://doi.org/10.1007/s11696-020-01220-3
[66] M. Khodiev, U. Holikulov, A. Jumabaev, N. Issaoui, L. Nikolay Lvovich *et al.*, *J. Mol. Liq.*, **382**, 121960 (2023), https://doi.org/10.1016/j.molliq.2023.121960
[67] A. Demirpolat, F. Akman and A. S. Kazachenko, *Molecules*, **27**, 6129 (2022), https://doi.org/10.3390/molecules27186129
[68] T. Koopmans, *Physica*, **1**, 104 (1934), https://doi.org/10.1016/S0031-8914(34)90011-2
[69] R. G. Parr, R. A. Donnelly, M. Levy and W. E. Palke, *J. Chem. Phys.*, **68**, 3801 (1978), https://doi.org/10.1063/1.436185

[70] R. G. Parr, L. V. Szentpály and S. Liu, *J. Am. Chem. Soc.*, **121**, 1922 (1999), https://doi.org/10.1021/ja983494x
[71] A. S. Kazachenko, N. Issaoui, U. Holikulov, O. M. Al-Dossary, I. S. Ponomarev *et al.*, *Zeitsch. Physik. Chem.*, **238**, 89 (2024), https://doi.org/10.1515/zpch-2023-0345
[72] A. Jumabaev, U. Holikulov, H. Hushvaktov, N. Issaoui and A. Absanov, *J. Mol. Liq.*, **377**, 121552 (2023), https://doi.org/10.1016/j.molliq.2023.121552
[73] H. D. Lutz, W. Eckers and H. Haeuseler, *J. Mol. Struct.*, **80**, 221 (1982), https://doi.org/10.1016/0022-2860(82)87236-0
[74] M. Thirunavukkarasu, G. Balaji, S. Muthu, B. R. Raajaraman and P. Ramesh, *Chem. Data Coll.*, **31**, 100622 (2021), https://doi.org/10.1016/j.cdc.2020.100622
[75] A. Thamarai, R. Vadamalar, M. Raja, S. Muthu, B. Narayana *et al.*, *Spectrochim. Acta A: Mol. Biomol. Spectrosc.*, **226**, 117609 (2020), https://doi.org/10.1016/j.saa.2019.117609
[76] L. J. Bellamy and R. L. Williams, *Spectrochim. Acta*, **9**, 341 (1957), https://doi.org/10.1016/0371-1951(57)80149-0
[77] S. Sevvanthi, S. Muthu, S. Aayisha, P. Ramesh and M. Raja, *Chem. Data Coll.*, **30**, 100574 (2020), https://doi.org/10.1016/j.cdc.2020.100574
[78] Z. Demircioğlu, Ç. A. Kaştaş and O. Büyükgüngör, *Mol. Cryst. Liq. Cryst.*, **656**, 169 (2017), https://doi.org/10.1080/15421406.2017.1405660